

## Supporting Information

# Highly Efficient and Selectivity Controllable Aerobic Oxidation of Ethyl Lactate to Ethyl Pyruvate over $V_xO_y/NC$ Catalyst

Zonghui Liu, Jing Xu, Lei Cui, Na Liu, Bing Yan and Bing Xue\*

*Jiangsu Province Engineering Research Center of Biodegradable Materials, School of Petrochemical Engineering, Changzhou University, Changzhou 213164, Jiangsu, China*

### Characterization methods

The X-ray diffraction (XRD) patterns were measured on a D/max 2500 PC X-ray diffractometer (Rigaku) with a graphite monochromator using Ni-filtered Cu-K $\alpha$  radiation with a scan speed of 5°/min and a scan range of 5~80°. N<sub>2</sub> adsorption-desorption (ASAP 2020 instrument) were analyzed to determine the textural properties. The surface areas and pore size distributions were calculated by Brunauer–Emmet–Teller (BET) and DFT method, respectively. Scanning electron microscopy (SEM) was analyzed on a Supra 55 (Zeiss) microscope operating at 30 kV. Transmission electron microscopy (TEM) experiments were performed on a 2010 electron microscope (JEOL). X-ray photoelectron spectroscopy (XPS) was analyzed on ESCALAB 250XI spectrometer (Thermo) using Mg/Al anode as X-ray source. The H<sub>2</sub>-temperature-programmed reduction (TPR) was performed in self-made equipment with a TCD detector. The sample (ca. 150 mg) was first pretreated at 500 °C for 0.5 h under Ar (25mL/min), then decreased to 100 °C and switched to a flow of 5% H<sub>2</sub>/Ar. Finally, the temperature increased to 900 °C at a heating rate of 15 °C/min. The water was removed by using ethanol/liquid nitrogen (-116 °C) before reaction gas enters the TCD detector.

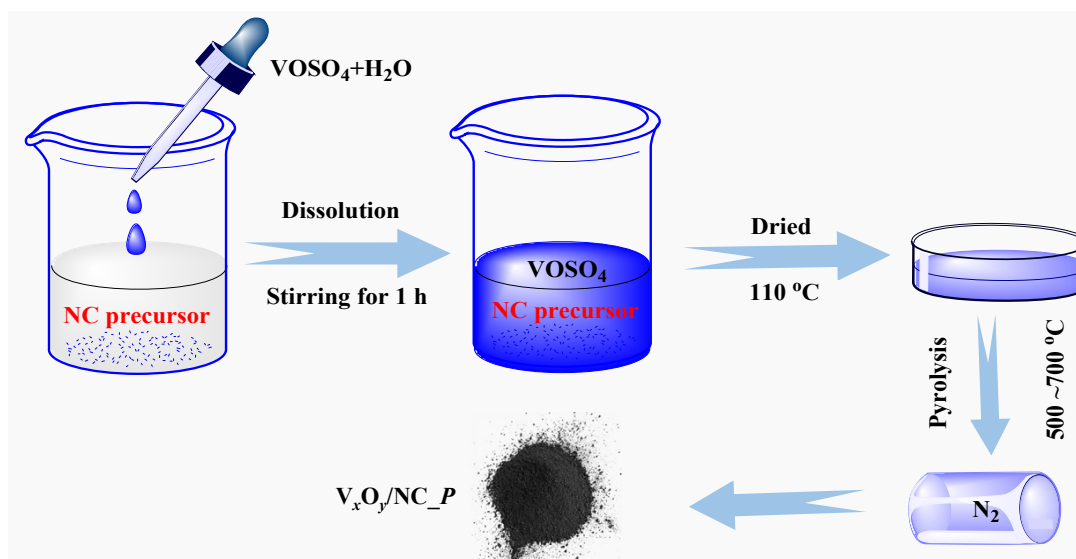


**Figure S1.** Schematic diagram for preparing  $V_xO_y/NC\_P$  catalyst

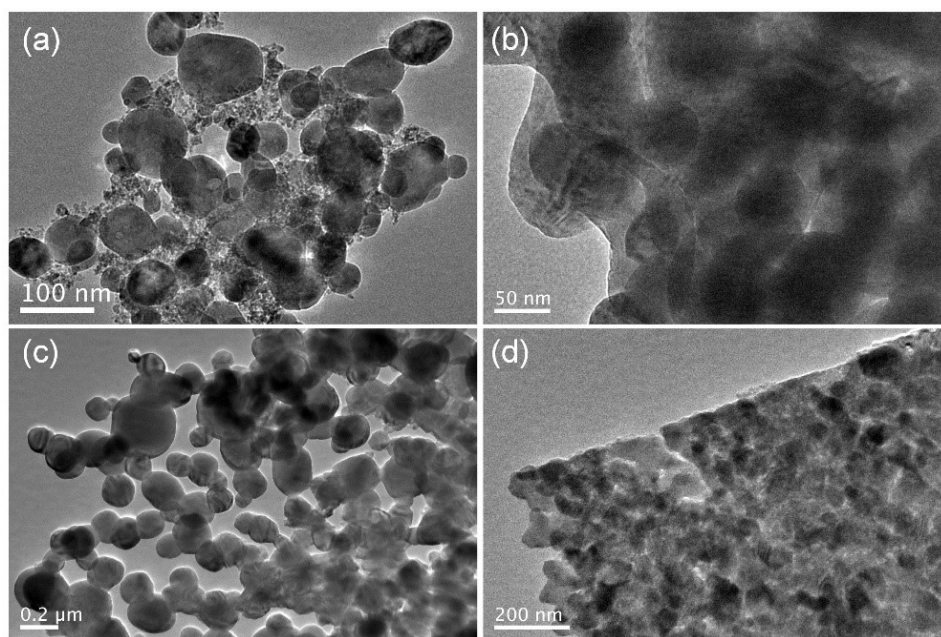


**Figure S2.** TEM image of  $V_xO_y/NC\_Melamine$  (a),  $V_xO_y/NC\_DCDA$  (b),  $V_xO_y/NC\_Urea$  (c)和  $V_xO_y/NC\_Methenamine$  (d)

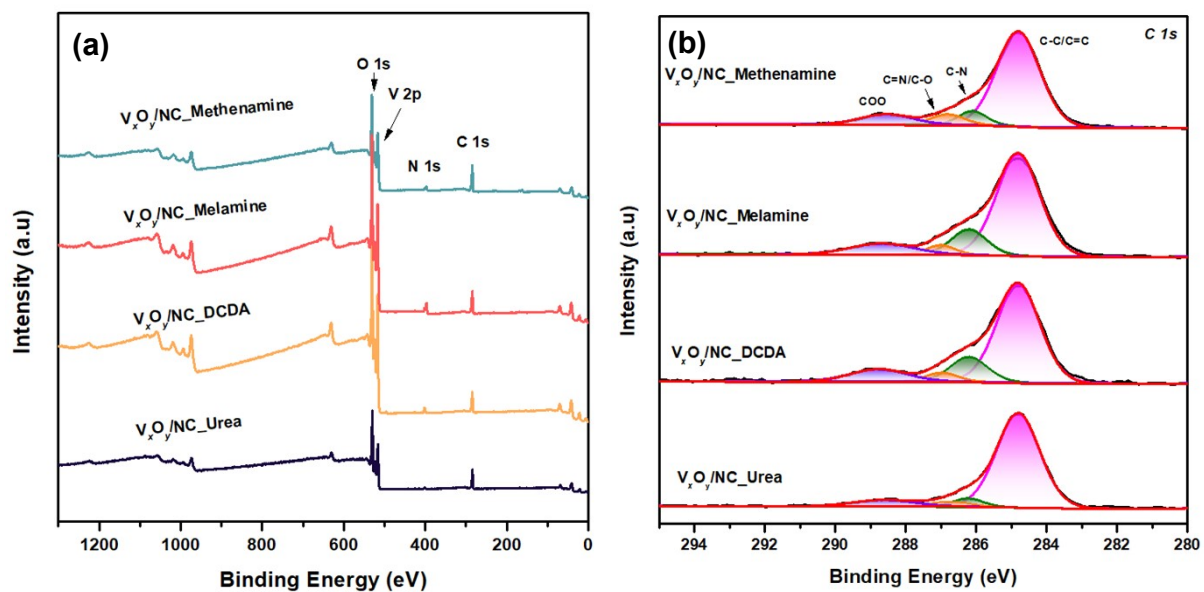


Figure S3. XPS survey spectra (a) of catalysts, and the high-resolution C1s (b)

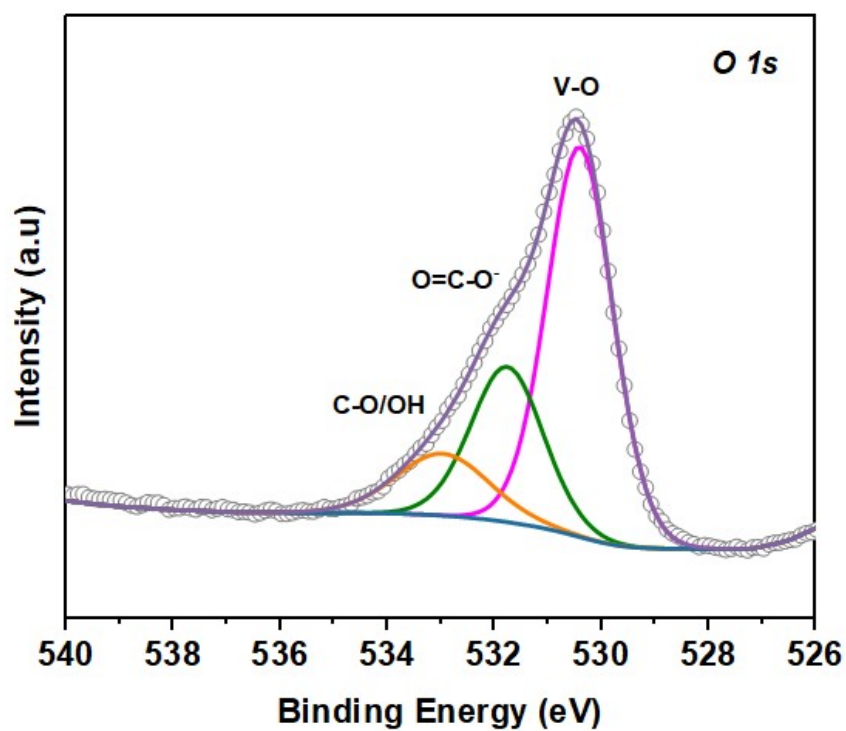


Figure S4. The high-resolution O1s of  $V_xO_y/NC\_Methenamine$

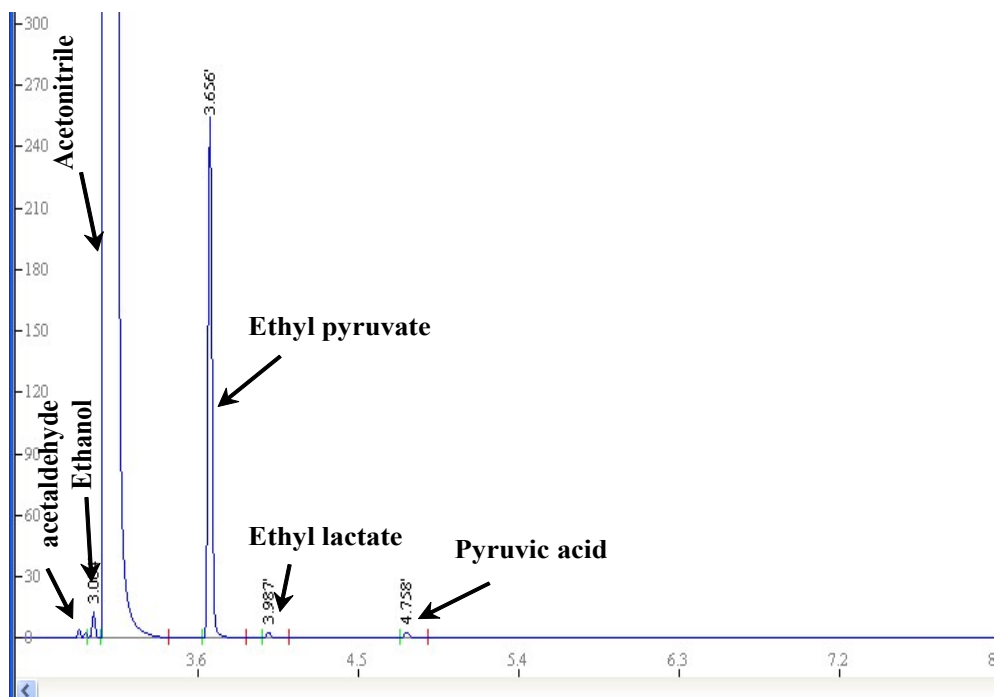


Figure S5. The GC-FID spectra of the EL conversion over  $V_xO_y/NC\_Methenamine$  catalyst.

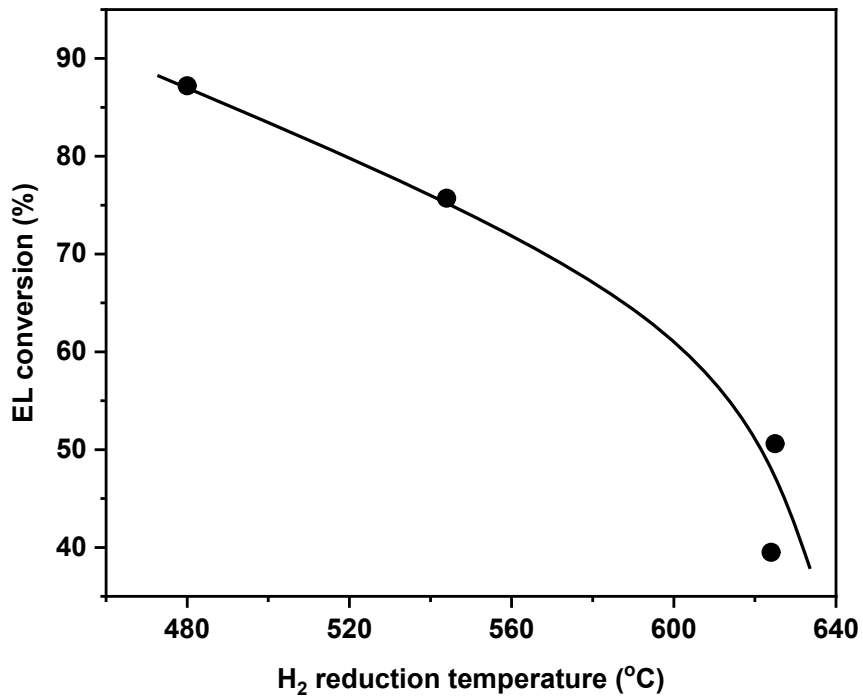
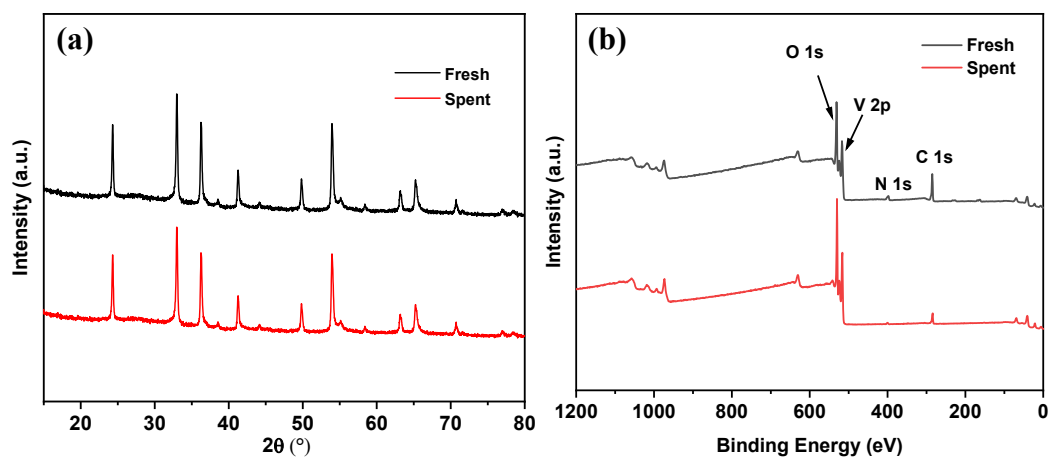


Figure S6. Relationship between catalytic activity and  $H_2$  reduction temperature.



**Figure S7.** XRD (a) and XPS survey spectra (b) of fresh and spent  $V_xO_y/NC$ \_Methenamine catalyst